Journal of Science and Engineering Papers
Volume: 03, Issue: 01 (January), 2026, page: 159-167
Journal homepage: www.jsciengpap.com
https://doi.org/10.62275/josep.24.1000001
ISSN: 3006-3191 (online), 3079-8175 (print)

Comparative Catalytic Efficiency and Polycondensation Kinetics of Succinic Acid and 1,3-Propanediol: A Kinetic Study of p-Toluene sulfonic Acid (p-TSA) versus $AlCl_3$

Md. Anwarul Karim*, **and Md. Abu Bakr**

Department of Applied Chemistry and Chemical Engineering, University of Rajshahi, Rajshahi-6205, Bangladesh.
*Corresponding author: e-mail address: makarim72@ru.ac.bd; ORCID: https://orcid.org/0000-0001-7538-6372

ARTICLE INFO

Received: 28th December, 2025
Revised: 17th January, 2026
Accepted: 18th January, 2026

Keywords:

p-TSA, $AlCl_3$,
polycondensation,
succinic acid,
1,3-propane diol,
poly(trimethylenesuccinate),
catalysis, polyesterification

ABSTRACT

This study presents a comparative investigation of two common catalysts - p-toluene sulfonic acid (p-TSA, a strong organic Brønsted acid) and aluminum chloride ($AlCl_3$, a Lewis acid) over non-catalyst one in the polycondensation of succinic acid (SA) with 1,3-propane diol (PDO) to form poly (trimethylene succinate) (PTSu). Reaction parameters (temperature, catalyst loading, and time) were systematically varied to evaluate catalyst efficiency with respect to (i) degree of polymerization, (ii) the rate of reaction of polycondensation, (iii) esterification rate, (iv) order of the reaction, and (v) activation energy of the reaction. Analytical techniques included FTIR & ^1H NMR. Mechanistic differences between Brønsted and Lewis acid catalysis are discussed. Results (representative data and trends are provided) indicate that p-TSA yields faster initial esterification and higher final molecular weights under identical conditions. In contrast, the $AlCl_3$ catalyst exhibits similar activity to the p-TSA catalyst. Among the non-catalyst, p-TSA, and $AlCl_3$ catalysts, the p-TSA and $AlCl_3$ catalysts performed well in the polycondensation reaction over the non-catalyst one.

1. Introduction

In recent decades, challenges related to waste management and environmental contamination from bio-resistant synthetic plastics have intensified. Many countries now prioritize the reuse and recycling of plastic waste. The development of biodegradable polymers offers an alternative solution to these issues. Currently, biodegradable polymers are used across various industries, including packaging, agriculture, sanitation, and biomedical applications. Among these materials, the aliphatic polyester family is considered particularly promising due to its susceptibility to biological degradation [1]. Consequently, additional research has focused on aliphatic polyesters synthesized through the polycondensation of dicarboxylic acids and diols.

In 1931, Carothers [2] synthesized and classified several aliphatic polyesters derived from diacids and diols, noting the challenges of producing high-molecular-weight polyesters at the time. From the 1930s to the 1990s, research on aliphatic polyesters was limited due to their inferior mechanical properties and higher costs compared to conventional plastics, rendering them unsuitable for engineering applications. Following the 1990s, increased environmental concerns stimulated renewed interest in aliphatic polyesters. Advances in chain extenders, high-vacuum technologies, and efficient transesterification catalysts have since enabled the synthesis of high-molecular-weight aliphatic polyesters with improved mechanical properties.

In 1990, Showa Highpolymer Co., Ltd. used polyfunctional isocyanate as a chain extender and organic compounds containing phosphorus and metals as reactive catalysts to commercialize specific aliphatic polyesters with molecular weights ranging from several tens of thousands to several hundred thousand [3–6]. These products are marketed under the BIONOLLE trademark. Among these, only poly(ethylene succinate) (PES) and poly(butylene succinate) (PBS) display melt temperatures above 100 °C (Tm approximately 108 °C and 114 °C, respectively) [7]. Consequently, many research groups have focused on PES [8–14] and PBS to improve their physical properties while maintaining biodegradability. One method of changing the characteristics of biodegradable PES and PBS was to create copolymers by adding various diacids or diols [15–29]. Additionally, biodegradability and its connection to polyesters' molecular weight and chemical structure were examined [28–31].

Previously, 1,3-propanediol's use was limited by low yield and high cost. Recent advances in production methods are expected to address these challenges [32–34]. Aliphatic copolyesters with odd-numbered carbon atoms in their backbone were seldom studied due to poor mechanical and thermal properties and a lack of crystallinity. However, Bikiaris' lab recently synthesized PES, PBS, and poly(trimethylene succinate) (PTS) with average molecular weights of 6800–6900 g/mol using polycondensation [12–14]. Investigating the morphology, odd-even effects, thermal properties, and crystallinity of these copolyesters is of significant interest.

Aliphatic polyesters represent the most extensively researched and produced category among biodegradable materials. Based on chemical structure, these polyesters are classified into two groups: those derived from hydroxy acids and those synthesized from alkanediols and aliphatic dicarboxylic acids. The former group is typically prepared by ring-opening polymerization, whereas the latter is typically synthesized by polycondensation. Three primary polycondensation approaches have been investigated: transesterification of aliphatic diols with dimethyl esters of dicarboxylic acids, esterification of aliphatic diols with dicarboxylic acids, and polycondensation of alkanediols with dichlorides of dicarboxylic acids in solution. Although the final method incurs higher costs during scale-up, it offers greater adaptability.

In this study, the polycondensation of succinic acid with 1,3-propanediol in equimolar ratios has been investigated in the absence and presence of p-toluene acid (p-TS) & AlCl3 as catalysts. The kinetic studies of the uncatalyzed and catalyzed reactions were analyzed using integration and graphical methods at various temperatures. The degree of polymerization (DPn) in the uncatalyzed, (p-TS) catalyst, and $AlCl_3$ catalyst reaction was also investigated and compared. The activation energy has also been examined accordingly. Finally, find out the suitable catalyst and conditions in the polycondensation of succinic acid and 1,3-propanediol.

2. Materials and methods

2.1. Materials

Materials: Succinic acid (⩾99% purity, E. Merck, Germany), 1,3-Propanediol (⩾ 99% purity, BDH Chemicals Ltd., England), p-Toluene Sulphonic Acid (p-TSA), (⩾98% purity, BDH Chemicals Ltd., England), Aluminum Chloride ($AlCl_3$) anhydrous (BDH Chemicals Ltd., England), Ethyl alcohol (Absolute, Cerew & Co. Bangladesh), Acetone (⩾99% purity, BDH Chemicals Ltd., England), Potassium hydroxide (⩾85% purity, Riedel-de Haen, Germany), Phenolphthalein (BDH Chemicals Ltd., England).

2.2. Preparation of polymer

The stoichiometric amounts of succinic acid and 1,3-propanediol were taken in a 50 ml beaker (0.4 mol% of p-TSA or AlCl3 used as a catalyst). The mixture was vigorously stirred to ensure it was well mixed. The reaction flask was connected to the vacuum pump to eliminate the byproduct water. The reaction mixture was heated with a heating mantle at a constant temperature of 160 ^{0}C. The constant temperature was maintained until bubbling started first. Then varying the time from 0 to 120 minutes with 15 minutes interval, such as starting from 30,45,60,76, 90, 105, and 120 minutes duration, maintained in non-catalyst, p-TSA catalyst, and $AlCl_3$. The obtained copolyester was dissolved in a minimum amount of alcohol and reprecipitated with a 10-fold amount of ice-cold methanol, using vigorous stirring. The reaction mixture was filtered, washed with methanol, and the precipitate was then dried at 60 °C in a vacuum oven for 24 h. The product obtained was a white solid, and the yield was 95%. The unreacted acid was titrated with standard alcoholic KOH solution using Phenolphthalein as an indicator.

2.3. Characterizations: The polymerization was characterized by measuring the degree of polymerization, FTIR, and NMR. The kinetics were measured by the rate of reaction and the order of the reaction.

2.4. Degree of polymerization

Degree of polymerization: The number of repeating units in the polymer chain is called the degree of polymerization. It is denoted by DPn.

$$DP_n = \frac{C_0}{C} \tag{1}$$

Where C_0 is the initial concentration of carboxyl groups, and C is the final concentration of unreacted carboxyl groups. It is convenient to introduce the extent of reaction, P, defined as the fraction of the functional groups that have reacted at time t, then we may write

$$C = C_0(1-P) \tag{2}$$

$$P = \frac{(C_0-C)}{C_0} \approx \frac{(V_0-V)}{V_0} \tag{3}$$

and $\frac{V_0}{V} = \frac{C_0}{C} = \frac{1}{(1-P)} = DP_n$ **(4)**

Therefore, $DP_n 1 \frac{V_0}{V_1}$, $DP_n 2 = \frac{V_0}{V_2}$ …etc.

V_0 is the volume of KOH that is consumed initially, and successive volumes after time: t_1, t_2, t_3, … etc. are V_1, V_2, V_3…… etc.

2.4. Determination of reaction rate

To calculate the rate of reaction from a graph, use the general formula: change in concentration divided by change in time.To find the average rate of a reaction, calculate the change in concentration divided by the change in time between the start and end of the reaction. The instantaneous rate is determined by finding the slope of the tangent to the concentration vs. time curve at a specific point, representing the rate at that exact moment. The initial rate is found using the change in concentration and the time interval between the initial concentration and the first measured data point after reaction begins.

The rate of a chemical reaction, or its speed or velocity, is defined as the rate at which concentrations of reacting species change with time and is denoted by $\frac{dc}{dt}$. Where C is the concentration of any reaction substance, and t is time. If the concentration of the reacting substance decreases with an increase in the reaction time, as in the case of reactants, the minus sign is put before dc/dt, i.e., -dc/dt is used. But if concentration increases with time, a plus sign is put before dc/dt.

If V_0 is the volume of KOH that is consumed initially, and successive volumes after time t_1, t_2, t_3, ……………..etc. are

https://doi.org/10.62275/josep.26.1000025

V_1, V_2, V_3......................etc., the reaction rate $-\frac{dv_1}{dt_1}, -\frac{dv_2}{dt_2}, -\frac{dv_3}{dt_3}$

$dV_1 = V_0 - V_1, dV_2 = V_1 - V_2, \ dV_3 = V_3 - V_2$

$dt_1 = t_1 - t_0, \ dt_2 = t_2 - t_1, \ dt_3 = t_3 - t_2$

2.5. Determination of reaction order

The order of a chemical reaction defines the functional relationship between reactant concentrations and the reaction rate. It can only be determined through experimental measurements, as it cannot be reliably predicted from balanced chemical equations. The most common method involves measuring the initial reaction rate across multiple experiments with varying starting concentrations. By observing how the rate changes relative to concentration changes, the partial order for each reactant is determined. Zero Order: Doubling the concentration does not affect the rate. First Order: Doubling the concentration doubles the rate. Second Order: Doubling the concentration quadruples the rate (increases by 2^2).

2.6. Integrated Rate Law Method

Experimental data is fitted into different integrated rate equations (mathematical models) to see which one yields a constant value for the rate constant (k). The number of reacting molecules whose concentration alters as a result of the chemical change is termed the order of the reaction. It is denoted by n. The order can be determined by the integration method, but this is a method of trial and error. The order of the reaction was determined by these equations, which give a satisfactory constant value of the velocity constant k.

For the first-order reaction,

$$k = \frac{1}{t} ln\left(\frac{C_0}{C}\right) \quad \textbf{(5)}$$

For the second-order reaction,

$$k = \frac{1}{t}\left(\frac{1}{C} - \frac{1}{C_0}\right) \quad \textbf{(6)}$$

For the third-order reaction,

$$k = \frac{1}{2t}\left(\frac{1}{C^2} - \frac{1}{C_0^2}\right) \quad \textbf{(7)}$$

Vant Hoff's differential method is more convenient. For a reaction of the n th order with the initial concentration.

$$-\frac{dc}{dt} = kc^n \quad \textbf{(8)}$$

$$\text{Or } log\left(-\frac{dc}{dt}\right) = logk + nlogc \quad \textbf{(9)}$$

The values of $C \approx V$ (volume of alcoholic KOH solution) was plotted against time t and dc/dt for any concentration, and time was determined from this curve. The logarithm of the rate (-dc/dt) was plotted against the corresponding logarithm value of $C \approx V$ (volume of alcoholic KOH solution), and a linear curve was obtained. The reaction order, n, was measured from the slope of this linear plot.

2.7. Determination of the velocity constant (Esterification rate constant)

The velocity constant k, used in the rate equation, is numerically equal to the reaction rate (−dc/dt) when all reactant concentrations are at unity (1 mol/L). For the second-order reaction, we know,

$$kt = \frac{1}{C} - \frac{1}{C_0}$$

$$\text{Or } \frac{1}{C} = kt + \frac{1}{C_0} \quad \textbf{(10)}$$

Where C_0 is the initial concentration of carboxyl groups (i.e., volumes of alc. KOH solution, V_0, that are initially consumed) and C is the unreacted carboxyl groups after time, t (i.e., volumes of alc. KOH solution, v that are consumed after time, t). The volumes of $1/C \approx 1/V$ are plotted against their corresponding time t, and a linear curve is obtained. The esterification rate constant k is measured from the slope of this linear plot.

For the third-order reaction, we know,

$$2kt = \frac{1}{C^2} - \frac{1}{C_0^2}$$

$$\text{Or } \frac{1}{C^2} = 2kt + \frac{1}{C_0^2} \quad \textbf{(11)}$$

The values of $1/C^2 \approx 1/V^2$ is plotted against its corresponding time, t, and a linear curve was obtained. The esterification rate constant, k, is measured from the slope of this linear plot.

2.8. Determination of energy of activation using Arrhenius equation

In slightly rearranged form from Arrhenius $lnk = \frac{E_a}{RT} + constant\ (lnA)$ can be written as

$$logk = -\frac{E_a}{2.303RT} + logA \quad \textbf{(12)}$$

According to the equation, a plot of log k versus 1/T should be a straight line with a slope $\frac{-E_a}{2.303RT}$ and intercept log A. Knowing the slope, the value of the constant E_a, which is characteristic of the reaction, can be calculated. Ea can also be determined if the specific rate constants are known at two different temperatures. If k_1 is the specific rate constant at temperature T_1 and k_2 is the specific rate constant at another temperature T_2, then from equations.

$$\log\frac{k_2}{k_1} = \frac{E_a}{2.303R}\left[\frac{T_2 - T_1}{T_1 T_2}\right] \quad \textbf{(13)}$$

It is evident from this equation that if the specific rate constants at two different temperatures are known, E_a can be readily evaluated or calculated.

3. Result and discussion

The following **scheme 1** represents the condensation polymerization reaction between succinic acid and 1,3-propanediol.

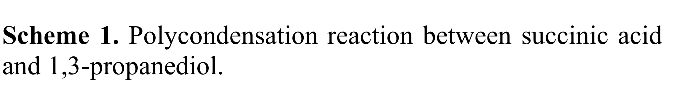

Scheme 1. Polycondensation reaction between succinic acid and 1,3-propanediol.

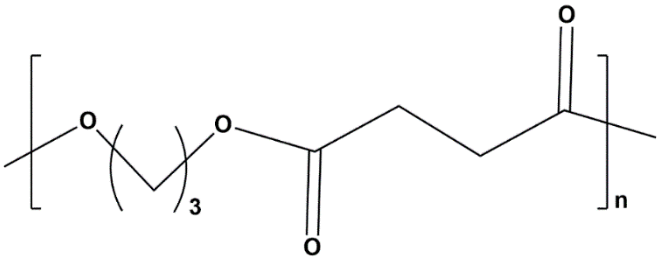

Figure 1. The structure of poly (tri-methylene succinate)

^{1}H Nuclear Magnetic Resonance Spectroscopy: The materials' ^{1}H nuclear magnetic resonance (NMR) spectra were captured using a Bruker AVANCE-III 500 MHz spectrometer (Billerica, MA, USA). The materials were dissolved in room-temperature Deuterated Chloroform ($CDCl_3$) solvent in 5 mm NMR tubes. **Figure 1** shows the structural configuration of the polymer. The polymer structure was confirmed by ^{1}H NMR spectroscopy below.

^{1}H NMR spectrum (CDCl3, 500 MHz, 25 ^{0}C): δ 5.12 (m, 1H); 4.17-4.14 (dd, J = 3.8, 11.5 Hz, 1H); 4.08-4.05 (dd, J = 6.3, 11.5 Hz, 1H); 2.61 (bm, 4H); 1.22 (d, J = 6.3, 3H)

δ5.12 (m, 1H): A multiplet integrating to one proton. The downfield shift suggests a proton attached to a carbon bearing an electronegative group, likely an oxygen (methine proton of an ester or alcohol). δ4.17-4.14 (dd, J = 3.8, 11.5 Hz, 1H) and δ 4.08-4.05 (dd, J = 6.3, 11.5 Hz, 1H): These two signals represent diastereotopic protons of a methylene group ($-CH_2-$), typically adjacent to a chiral center. The large coupling constant (J = 11.5 Hz) is characteristic of geminal coupling ($^2J_{HH}$). The smaller couplings (3.8 Hz and 6.3 Hz) represent vicinal coupling ($^3J_{HH}$) to the proton at δ 5.12.

δ 2.61 (bm, 4H): A broad multiplet integrating to four protons. This pattern is often seen in ethylene groups ($-CH_2CH_2-$) within a ring or adjacent to carbonyl groups (e.g., in a succinate or similar moiety).

δ1.22 (d, J = 6.3 Hz, 3H): A doublet integrating to three protons, characteristic of a methyl group ($-CH_3$) coupled to a single methine proton. The coupling constant (6.3 Hz) matches one of the vicinal couplings seen in the downfield signals, confirming its proximity to the proton at δ 5.12.

The data is highly consistent with a 1,2-propanediol derivative, such as a cyclic ester or a substituted glycerol fragment. Specifically, the spin system $CH_3-CH(O-)-CH_2O-$ is clearly defined by the couplings between the signals at δ 1.22, 5.12, and the pair at 4.15/4.06.

Table1. Summarized the FTIR spectrum

Functional group	Wavenumber range	Assignment
$C=O$	~1716-1747 cm^{-1}	Carbonyl stretching vibration (ester group)
$C-H$	~2800-3000 cm^{-1}	C-H stretching vibrations (from the trimethylene segment)
$C-O$	~1040-1255 cm^{-1}	C-O ester bond symmetric and asymmetric stretching
CH_2 / CH_3	~1350-1470 cm^{-1}	Bending and scissoring vibrations of methylene/methyl groups

Fourier Transform Infrared Spectroscopy: Using a PerkinElmer Spectrum One FT-IR spectrometer (ATR testing model) in the transmission mode in the range of 4000−650 cm^{-1} with a resolution of 4 cm^{-1}, 16 scans were used to describe the chemical structure of the synthesized Poly(trimethylene succinate) (**PTSu**).

The absorption bands associated with both the succinic acid and trimethylene segments shift slightly depending on the polymer's phase (amorphous or crystalline). The primary functional groups and their corresponding approximate absorption ranges are listed in **Table1.** The Absence of a broad –OH band near 3300 cm^{-1} indicates successful condensation.

Degree of polymerization: Poly(propylene succinate), formed by condensation polymerization of succinic acid and 1,3-propanediol, typically achieves degrees of polymerization corresponding to the monomer starting from 1.757, depending on reaction conditions like temperature, catalyst, and time. The higher DP_n of up to 9,277 has been reported for the final polyester in this study. Condensation polymerization occurs via melt polycondensation, often in bulk at 150–200°C, removing water to drive the equilibrium toward higher chains. The polycondensation of succinic acid with 1,3-propanediol in equimolar ratios has been investigated in bulk at 120-160^{0}C in the absence and presence of p-toluene acid (p-TSA) & $AlCl_3$ as catalysts.

The kinetic studies were investigated. The rate constants for the uncatalyzed and catalyzed reactions were analyzed using integration and graphical methods at various temperatures. The activation energy has also been determined. From the investigation results, it was observed that the degree of polymerization (DP_n) in the uncatalyzed reaction is the square root of that obtained in the p-TSA-catalyzed reaction and the DPn obtained in the $AlCl_3$-catalyzed reaction. But the degree of polymerization obtained in the $AlCl_3$-catalyzed reaction is almost similar to that of p-TSA-catalyzed polymerization, as shown in **Figure 2**. Catalysts like p-TSA (p-toluene sulfonic acid) and $AlCl_3$ significantly enhance the rate of step-growth

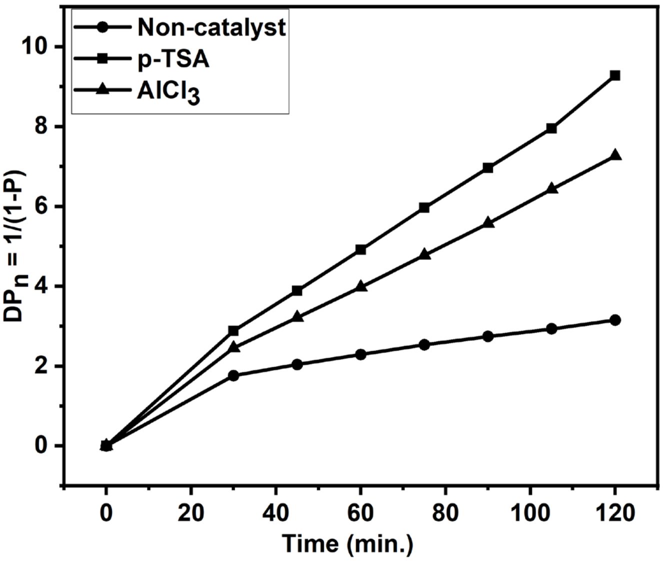

Figure 2. Degree of polymerization with non-catalyst, p-TSA, and $AlCl_3$

polycondensation reactions, such as polyesterification, compared to uncatalyzed processes, as shown in **Figure 3.**

The p-TSA, a Brønsted acid, initiates polycondensation (e.g., polyesterification) by protonating the carbonyl oxygen of carboxylic acid groups, enhancing electrophilicity for nucleophilic attack by alcohol hydroxyls to form esters and water. The $AlCl_3$, a Lewis acid, primarily initiates cationic vinyl polymerizations by coordinating to monomer double bonds or impurities (e.g., water), generating carbocations that propagate chain growth. In shared contexts like polyesterification, both are catalysed via acid activation, but differ in the strength of their mechanism and coordination mode [37]. This acceleration allows the reaction to reach higher conversions (p closer to 1), directly increasing the degree of polymerization (DPn) via Carothers' equation:

$$DP_n = \frac{1}{(1-P)} \quad \textbf{(14)}$$

The reaction rates for the non-catalysed, p-TSA-catalysed, and $AlCl_3$-catalyzed polycondensations between succinic acid and 1,3-propanediol at 160 ^{0}C were investigated. The graphical representations of these are shown in **Figure 3.** It has been seen that the rate of reaction of p-TSA-catalysed is much faster than that of the non-catalysed one. But the rate of reaction with $AlCl_3$-catalyzed polycondensation is almost similar to that of p-TSA catalyst. The $AlCl_3$ and p-TSA catalysed polycondensation through distinct mechanisms, the Lewis acid coordination versus Brønsted acid protonation, but achieve comparable rates by similarly activating carbonyl groups in monomers like diacids and diols [38]. The p-TSA protonates the carbonyl oxygen of the carboxylic acid, forming a highly electrophilic protonated species that facilitates nucleophilic attack by the alcohol hydroxyl group. Proton transfer to the departing water molecule regenerates neutral p-TSA, completing the cycle; this process repeats efficiently in high-temperature melts with vacuum-driven water removal. The $AlCl_3$ binds directly to the carbonyl oxygen via dative bonding, polarizing the C=O bond and creating a Lewis acid-activated complex akin to protonation in electrophilicity. Nucleophilic addition forms a tetrahedral intermediate, followed by elimination of water and dissociation of $AlCl_3$, which recycles by coordinating fresh monomer; Chloride ligands may modulate activity but do not hinder turnover [40]. The comparison of p-TSA and $AlCl_3$ catalysts in the cycle at different aspect are summarized in **Table 2.**

Table 2. The comparison of p-TSA and $AlCl_3$ catalysts in the cycle at different aspects

Aspect	**p-TSA (Brønsted)**	**$AlCl_3$ (Lewis)**
Activation Mode	Protonation of O	Coordination to O
Key Intermediate	Protonated carbonyl	Lewis adduct/tetrahedral
Regeneration	Proton handover to byproduct	Dissociation from the product
Sensitivity	To water (reversible)	To hydrolysis (adduct formation)
Rate Equivalence	Fast proton mobility	Strong polarization matches

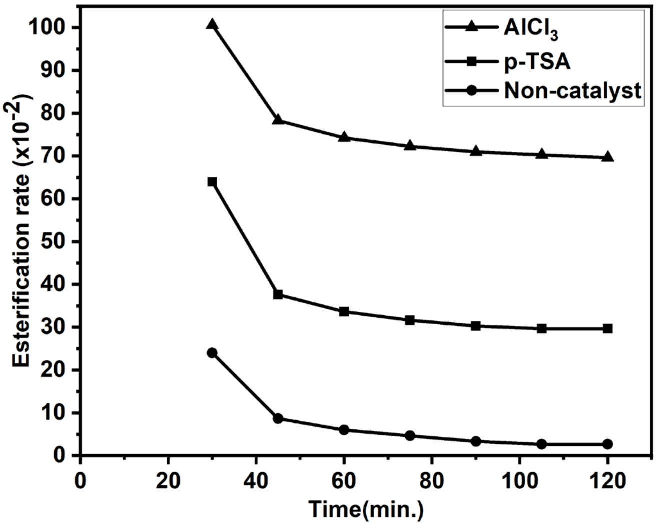

Figure 3. The rate of esterification at different time durations with non-catalyst, p-TSA, and $AlCl_3$ catalyzed system.

In uncatalyzed polycondensation, such as between a diacid and diol, the reaction requires simultaneous collision of three species: two monomers and a water molecule displaced in the reverse direction, or effectively ternary encounters in the rate-determining step. This leads to third-order kinetics as shown in **Figure 4,** typically expressed as rate = k [monomer]^2 [chain end] or similar, where chain growth depends on bifunctional interactions without facilitation [43].

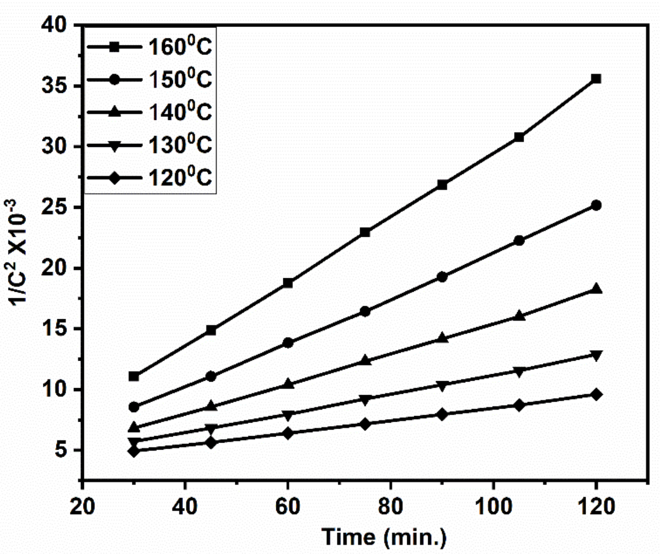

Figure 4. The third-order non-catalyst reaction at different temperatures and times.

The p-TSA (p-toluenesulfonic acid) and $AlCl_3$ act as strong acids or Lewis acids, protonating or coordinating the carbonyl oxygen of succinic acid to form a highly electrophilic intermediate. This activated species then undergoes nucleophilic attack by the alcohol from 1,3-propanediol in a bimolecular step, reducing the order to second (rate = k [activated acid] [alcohol]) as shown in **Figure 5** and **Figure 6.** Catalysts lower the activation energy and decouple the process from ternary collisions [44]. Uncatalyzed relies on direct monomer-monomer interactions needing three-body collisions; catalysis creates a steady-state activated monomer, making it binary.

https://doi.org/10.62275/josep.26.1000025

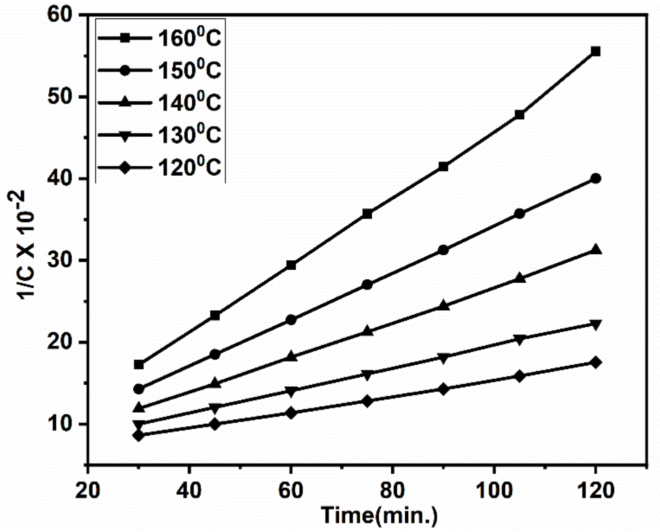

Figure 5. The second-order p-TSA catalyst reaction at different temperatures and times.

Activation energies for the condensation polymerization of succinic acid and 1,3-propanediol vary by catalyst and are typically determined via integral methods analyzing reaction rates at different temperatures. No direct Arrhenius plots exist in literature for the exact condensation polymerization of succinic acid and 1,3-propanediol (PPSu) using the integration method across non-catalyzed, p-TSA, and $AlCl_3$ cases. The activation energies were calculated from lnk vs. 1/T plots as shown in **Figure 7**. Activation energy E_a follows the Arrhenius equation:

$$lnk = lnA - \frac{E_a}{RT} \tag{15}$$

where the slope of the linear plot $lnk\ vs.\ 1/T$ (in K^{-1}) equals $-E_a / R$ (R = 8.314 J/mol·K). The integration method converts time-conversion data to rate constants k at isothermal conditions. Activation energies for the polycondensation of succinic acid and 1,3-propanediol decrease with catalysts like p-TSA or $AlCl_3$ compared to the uncatalyzed reaction, as catalysts lower the energy barrier for esterification and chain growth steps. Activation energies for the polycondensation of succinic acid and 1,3-propanediol vary by catalyst, with catalysis generally lowering the barrier compared to uncatalyzed reactions. Specific values for p-TSA and $AlCl_3$ are scarce in the literature, but data for the uncatalyzed first step (esterification) and similar systems provide context for comparison. Lower activation energies indicate faster reaction rates under catalysis.

The graphical method for determining activation energy in condensation polymerization, such as between succinic acid and 1,3-propanediol, typically involves plotting the natural logarithm of the rate constant (ln k) versus the inverse of absolute temperature (1/T), known as the Arrhenius plot. The activation energy (Ea) is calculated from the slope of the linear fit, where slope = -Ea/R, and R is the gas constant (8.314 J/mol·K). This method applies to non-catalyzed, p-TSA-catalyzed (p-toluenesulfonic acid, a Brønsted acid catalyst), and $AlCl_3$-catalyzed (a Lewis acid catalyst) conditions. In these reactions, catalysts typically lower the activation energy (Ea) by stabilizing the transition state during esterification and polycondensation, as illustrated in **Figure 8**.

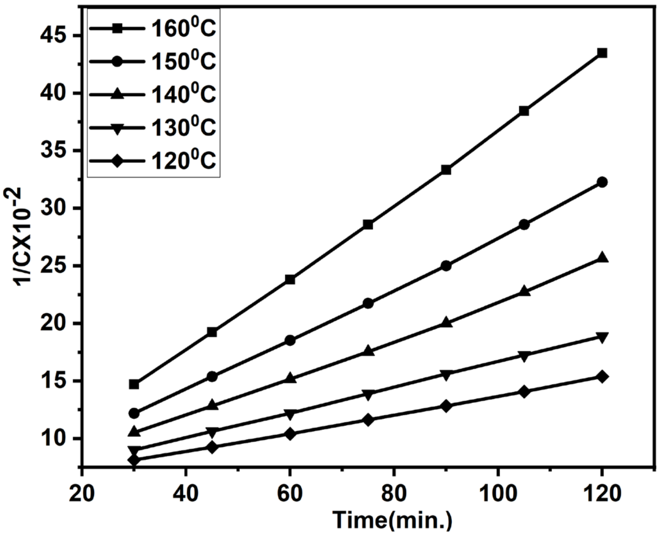

Figure 6. The second-order $AlCl_3$ catalyst reaction at different temperatures and times.

In condensation polymerization, rate constants are derived from experimental data on water evolution, monomer conversion, or molecular weight growth at varying temperatures. For non-catalyzed reactions, Ea is higher due to reliance on uncatalyzed proton transfers; p-TSA reduces Ea by providing protons for nucleophilic attack on carbonyls; $AlCl_3$ further lowers it via coordination to oxygen, enhancing electrophilicity.

Effects of Non-catalyst on Ea reflect high energy barriers for diacid-diol esterification. The effects of p-TSA catalyst on Ea drops as sulfonic acid accelerates carboxyl activation. The effects of $AlCl_3$ catalyst- Lowest Ea from strong Lewis acid coordination, reducing nucleophilic attack barriers.
$AlCl_3$ and p-TSA pathways in melt polycondensation exhibit comparable activation energies due to equivalent carbonyl activation strengths, despite mechanistic differences, leading to similar observed reaction rates [41]. The studies show that Lewis acid ($AlCl_3$) coordination to the carbonyl oxygen yields activation barriers closely matching those of Brønsted acid (p-TSA) protonation, as both polarize the C=O bond similarly (e.g., for esterification steps). Experimental kinetics in polyester melt reactions confirm this parity, with $AlCl_3$

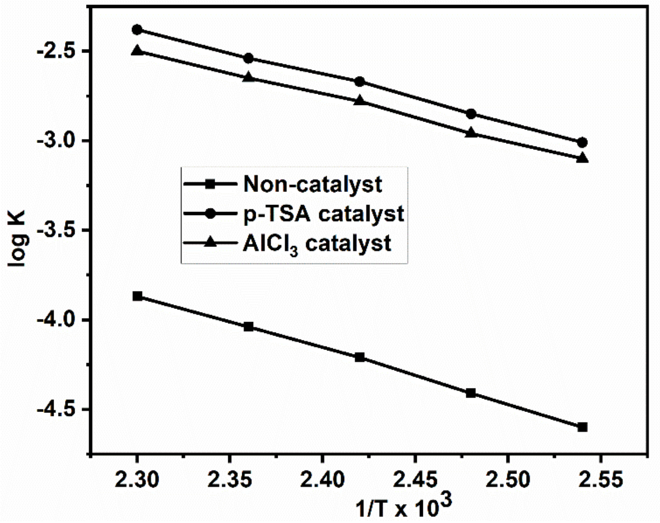

Figure 7. Activation energy in the integration method in the case of non-catalyst, p-TSA catalyst, and $AlCl_3$ catalyst.

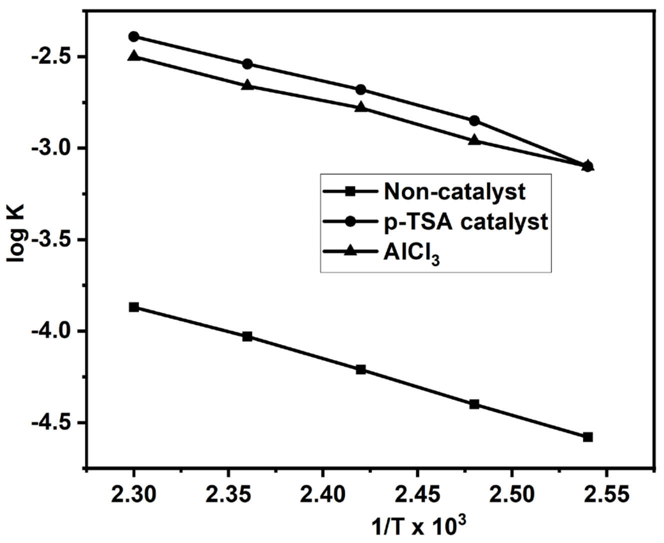

Figure 8. Activation energy in the graphical method in the case of non-catalyst, p-TSA catalyst, and AlCl$_3$ catalyst.

pathways sometimes slightly lower due to tighter coordination without proton transfer entropy losses [38].

The p-TSA protonation involves higher entropic penalties due to solvent-like proton mobility in melts, which are partially offset by rapid turnover. In contrast, the AlCl$_3$ rigid adduct lowers enthalpy barriers but risks compromising adduct stability. Overall, effective Ea aligns (e.g., reported for both in polycondensation), explaining the rate similarity with the uncatalyzed process.

Table 3 summarizes the implications for the rates of uncatalyzed, p-TSA-catalyzed, and AlCl$_3$-catalyzed reactions, as shown in **Figure 7** and **Figure 8.**

Table 3. Comparison of the activation energy for uncatalyzed, p-TSA-catalyzed, and AlCl$_3$-catalyzed in polycondensation.

Condition	Ea (kcal/mol) Integrated Method	Ea (kcal/mol) Graphical Method	Key barrier reduction
Non-catalyzed	13.728	13.694	Direct nucleophilic attack [41]
p-TSA	11.897	11.914	Protonated acylium formation [42]
AlCl$_3$	11.44	11.454	Lewis adduct polarization [38]

The mechanism involves the protonation of the carboxylic acid carbonyl oxygen (fast, low Ea), followed by nucleophilic addition by the alcohol (slow, Ea controlling the overall rate), and deprotonation/elimination of water (fast). This addition step governs kinetics due to steric and electronic barriers in the melt phase [39].

The analyses confirm that the transition state for C-O bond formation post-protonation has the highest barrier, as protonation alone lowers but does not eliminate repulsion between approaching groups. Vacuum removal of water accelerates subsequent steps, isolating this addition as rate-limiting, consistent with observed orders in polyesterification [38].

4. Conclusion

In this article, we compared the non-catalyst, p-TSA catalyst, and AlCl$_3$ catalyst performance, and kinetic studies were also compared in the polycondensation reaction between succinic acid and 1,3-propanediol to synthesize aliphatic biodegradable polyester. The NMR and FTIR analyses were used to confirm that the polymerization was successful. The degree of polymerization, rate of reaction, reaction order, esterification rate, and activation energy were investigated during polycondensation using three different catalysts: non-catalyst, p-TSA, and AlCl$_3$. Polycondensation generally proceeds via step-growth mechanisms with the removal of water to form ester linkages. Catalysts such as Lewis acids (e.g., AlCl$_3$) and Brønsted acids (e.g., p-toluene sulfonic acid) can significantly influence reaction kinetics, degree of polymerization, and lower activation energy. AlCl$_3$ functions by coordinating to carbonyl oxygens, enhancing electrophilicity, whereas p-TSA protonates carboxyls, accelerating ester formation. The investigated results reveal that the p-TSA catalyst and AlCl$_3$ have almost similar activities on the polycondensation reaction, but it is better than that of the non-catalyst one. These catalysts can be selected based on desired polymer properties for specific applications. The Poly(trimethylene succinate) (PTSu) is a biodegradable aliphatic polyester suitable for compostable films, controlled-release matrices, and potentially biomedical applications.

Reference

1. Mochizuki, M., Hirami, M.(2019). Structural effects on the biodegradation of aliphatic polyesters. Polymers for Advanced Technologies, 8:203–209. https://doi.org/10.1002/(SICI)1099-1581(199704)8:4<203::AID-PAT627>3.0.CO;2-3
2. Carothers, W.H. (1931). Polymerization. Chem Rev 8:353–425.
3. Takiyama, E., Harigai, N., Hokari, T.(1993). Production of aliphatic polyester. JP Patent H5-70566.
4. Takiyama, E., Seki, S.(1993). Production of aliphatic polyester. JP Patent H5-70572.
5. Takiyama, E., Fujimaki, T., Seki, S., Hokari, T., Hatano, Y. (1994). Method for manufacturing biodegradable high molecular aliphatic polyester. US Patent 5,310,782.
6. Takiyama, E., Hatano, Y., Fujimaki, T., Seki, S., Hokari, T., Hosogane, T., Harigai, N.(1995). Method of producing a high molecular weight aliphatic polyester and film thereof. US Patent 5,436,056.
7. Fujimaki, T.(1998). Processability and properties of aliphatic polyesters, ''BIONOLLE'', synthesized by polycondensation reaction. Polym. Degrad. Stab., 59:209–214.
8. Gan, Z., Abe, H., Doi, Y.(2000). Biodegradable poly(ethylene succinate) (PES) 1. Crystal growth kinetics and morphology. Biomacromolecules, 1:704–712.
9. Gan, Z., Abe, H., Doi, Y.(2000). Biodegradable poly(ethylene succinate) (PES) 2. Crystal morphology of melt-crystallized ultrathin film and its change after enzymatic degradation. Biomacromolecules, 1:713–720.

10. Qiu, Z., Ikehara, T., Nishi, T.(2003). Crystallization behaviour of biodegradable poly(ethylene succinate) from the amorphous state. Polymer, 44:5429–5437.
11. Qiu, Z., Komura, M., Ikehara, T., Nishi, T.(2003). DSC and TMDSC study of melting behaviour of poly(butylene succinate) and poly(ethylene succinate). Polymer, 44:7781–7785.
12. Papageorgiou, G.Z., Bikiaris, D.N.(2005). Crystallization and melting behavior of three biodegradable poly(alkylene succinates). A comparative study. Polymer, 46:12081–12092.
13. Bikiaris, D.N., Papageorgiou, G.Z., Achilias, D.S.(2006). Synthesis and comparative biodegradability studies of three poly(alkylene succinate)s. Polym. Degrad. Stab., 91:31–43.
14. Chrissafis, K., Paraskevopoulos, K.M., Bikiaris, D.N.(2005). Thermal degradation mechanism of poly(ethylene succinate) and poly(butylene succinate): comparative study. Thermochim Acta, 435:142–150.
15. Gan, Z., Abe, H., Doi, Y.(2001). Crystallization, melting, and enzymatic degradation of biodegradable poly(butylene succinate-co-14 mol% ethylene succinate) copolyester. Biomacromolecules, 2: 313–321.
16. Gan, Z., Abe, H., Kurokawa, H., Doi, Y. (2001). Solid-state microstructures, thermal properties, and crystallization of biodegradable poly(butylene succinate) (PBS) and its copolyesters. Biomacromolecules, 22:605–613.
17. Ahn, B.D., Kim, S.H., Kim, Y.H., Yang, J.S.(2001). Synthesis and characterization of the biodegradable copolymers from succinic acid and aliphatic acid with 1,4-butanediol. J. Appl. Polym. Sci., 82:2808–2826.
18. Nikolic, M.S., Djonlagic, J.(2001). Synthesis and characterization of biodegradable poly(butylene succinate-co-butylene adipate)s. Polym. Degrad. Stab., 74:263–270.
19. Kuwabara, K., Gan, Z., Nakamura, T., Abe, H., Doi, Y.(2002). Molecular mobility and phase structure of biodegradable poly(butylene succinate) and poly(butylene succinate-co-butylene adipate). Biomacromolecules, 3:1095–1100.
20. Zhu, C., Zhang, Z., Liu, Q., Wang, Z., Jin, J.(2003). Synthesis and biodegradation of aliphatic polyesters from dicarboxylic acids and diols. J. Appl. Polym. Sci., 90:982–990.
21. Cao, A., Okamura, T., Nakayama, K., Inoue, Y., Masuda, T.(2002). Studies on syntheses and physical properties of biodegradable aliphatic poly(butylene succinate-co-ethylene succinate)s and poly(butylene succinate-co-diethylene glycol succinate)s. Polym. Degrad. Stab., 8:107–117.
22. Cao, A., Okamura, T., Ishiguro, C., Nakayama, K., Inoue, Y., Masuda, T.(2002). Studies on syntheses and physical characterization of biodegradable aliphatic poly(butylene succinate-co-e-caprolactone)s. Polymer, 43:671–679.
23. Kim, M.N., Kim, K.H., Jin, H.J., Park, J.K., Yoon, J.S.(2001). Biodegradability of ethyl and n-octyl branched poly(ethylene adipate) and poly(butylene succinate). Eur. Polym. J., 37:1843–1847.
24. Chae, H.G., Park, S.H., Kim, B.C., Kim, D.K.(2004). Effect of methyl substitution of the ethylene unit on the physical properties of poly(butylene succinate). J. Polym. Sci. Part B: Polym. Phys., 42:1759–1766.
25. Oishi, A., Nakano, H., Fujita, K., Yuasa, M., Taguchi, Y.(2002). Copolymerization of poly(butylene succinate) with 3-alkoxy-1,2-propanediols. Polym. J. 34:742–747.
26. Mani, R., Bhattacharya, M., Leriche, C., Nie, L., Bassi, S.(2002). Synthesis and characterization of functional aliphatic copolyesters. J. Polym. Sci. Part A: Polym. Chem., 40:3232–9.
27. Nikolic, M.S., Poleti, D., Djonlagic, J. (2003). Synthesis and characterization of biodegradable poly(butylene succinate-co-butylene fumarate)s. Eur. Polym. J., 39:2183–92.
28. Mochizuki, M., Mukai, K., Yamada, K., Ichise, N., Murase, S., Iwaya, Y.(1997). Structure effects upon enzymatic hydrolysis of poly(butylene succinate-coethylene succinate)s. Macromolecules, 30:7403–7.
29. Rizzarelli, P., Puglisi, C., Montaudo, G.(2004). Soil burial and enzymatic degradation in solution of aliphatic co-polyesters. Polym. Degrad. Stab., 85:855–863.
30. Iwata, T., Doi, Y., Isono, K., Yoshida, Y.(2001). Morphology and enzymatic degradation of solution-grown single crystals of poly(ethylene succinate). Macromolecules, 34:7343–7348.
31. Cho, K., Lee, J., Kwon, K.(2001) Hydrolytic degradation behavior of poly(butylene succinate)s with different crystalline morphologies. J. Appl. Polym. Sci.,79:1025–1033.
32. Slaugh, L.H., Weider, P.R.(1993). Process for making 3-hydroxypropanal and 1,3-propanediol. US Patent 5,256,827.
33. Haynie, S.L., Wagner, L.W. (1997). Process for making 1,3-propanediol from carbohydrates using mixed microbial cultures. US Patent 5,599,689.
34. Emptage, M., Haynie, S.L., Laffend, L.A., Pucci, J.P., Whited, G.(2003). Process for the biological production of 1,3-propanediol with high titer. US Patent 6,514,733 B1.
35. Wu, C.-H., Chen, P.-H., Huang, Y.-L., Ranganathan, P., Rwei, S.-P., Chuan, F.-S.(2020). Solvent-Free One-Shot Synthesis of Thermoplastic Polyurethane Based on Bio-Poly(1,3-propylene succinate) Glycol with Temperature-Sensitive Shape Memory Behavior. ACS Omega, 5(8), 4058–4066,
36. Bikiaris, D.N., Papageorgiou, G.Z., Papadimitriou, S.A., Karavas, E., Avgoustakis, K.(2009). Novel Biodegradable Polyester Poly(Propylene Succinate): Synthesis and Application in the Preparation of Solid Dispersions and Nanoparticles of a Water-Soluble Drug. AAPS PharmSciTech, 10, 138–146.
37. Yokozawa, T., Yokoyama, A.(2007). Chain-growth polycondensation: The living polymerization process in polycondensation. Progress in Polymer Science. 32(1): 147-172.
38. Li, Q., Hunter, K.C., Allan L. L. East. A Theoretical Comparison of Lewis Acid vs Bronsted Acid Catalysis for n-Hexane → Propane + Propene. J. Phys. Chem. A, 109(28), 6223–6231.
39. Hans, R. K., Weidner, S.M., Falkenhagen, J.(2022). The role of transesterifications in reversible polycondensations and a reinvestigation of the Jacobson–Beckmann–Stockmayer experiments. Polym.. Chem., 13:1177-1185.
40. Schmallegger, M., Wiech, M., Soritz, S., Velásquez-Hernández, M.J., Bitschnau, B., Gruber-Woelfler, H., Gescheidt, G.(2025). Polystyrene-bound $AlCl_3$ - a catalyst for the solvent-free synthesis of aryl-substituted tetrazoles. Catal. Sci. Technol., 15(6):1983-1988.

41. Shigemoto, I., Kawakami, T., Taiko, H., Okumura, M.(2011). A quantum chemical study on the polycondensation reaction of polyesters: The mechanism of catalysis in the polycondensation reaction. Polymer. 52(15):3443-3450.
42. Khodabakhshi, S., Karami, B., Eskandari, K., Rashidi, A.(2015). A Facile and Practical p-Toluenesulfonic Acid Catalyzed Route to Dicoumarols Containing an Aroyl group. S. Afr. J. Chem., 68:53–56.
43. Szabó-Réthy, E.(1971). Comments on the calculation methods of kinetics of polyesterification reactions. European Polymer Journal. 7(10):1485-1499.
44. Philipp, A.M., Rajagopalan, B., Congalidis, J.P., Murphy, E.R.(2012). Mathematical Modeling of Acid-Catalyzed 1,3-Propanediol Polymerization. Macromol. React. Eng., 6:126–152.

Funding

The authors declare that no funds, grants, or other support were received during the preparation of this manuscript. The investigation was not funded by any organization or any sources.

Acknowledgement

Department of Applied Chemistry and Chemical Engineering, University of Rajshahi. Motihar, Rajshahi 6205, University of Rajshahi, Bangladesh.

Ethical Approval:

The submitted work is a unique contribution to the field, not published elsewhere in any form or language. Results are presented clearly, honestly, and without fabrication, falsification or inappropriate data manipulation (including image-based manipulation). Authors adhere to discipline-specific rules for acquiring, selecting and processing data.

Consent to Participate:

No human subject or living organism/tissue is involved in this investigation.

Consent to Publish:

No consent to publish is to be shared.

Author Contributions

All authors contributed to the study conception and design. Material preparation, data collection and analysis were performed by Md. Abu Bakr. The first draft of the manuscript was written by Md. Anwarul Karim and all authors commented on previous versions of the manuscript. All authors read and approved the final manuscript.

https://doi.org/10.62275/josep.26.1000025